

Fast Nonradiative Decay in *o*-Aminophenol

Marcela C. Capello,[†] Michel Broquier,^{‡,§} Shun-Ichi Ishiuchi,^{||} Woon Y. Sohn,^{||} Masaaki Fujii,^{||} Claude Dedonder-Lardeux,[⊥] Christophe Jovet,[⊥] and Gustavo A. Pino^{*,†}

[†]Instituto de Investigaciones en Físico Química de Córdoba (INFIQC) CONICET, UNC. Dpto. de Físicoquímica, Facultad de Ciencias Químicas, Centro Láser de Ciencias Moleculares, Universidad Nacional de Córdoba, Ciudad Universitaria, X5000HUA Córdoba, Argentina

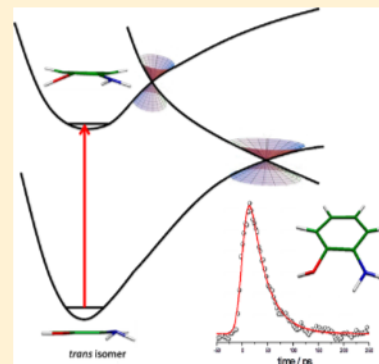
[‡]Centre Laser de l'Université Paris Sud (CLUPS, LUMAT FR 2764) Bât. 106, Univ Paris-Sud 11, 91405 Orsay Cedex, France

[§]Institut des Sciences Moléculaires d'Orsay (ISMO, UMR8624 CNRS) Bât. 210, Univ Paris-Sud 11, 91405 Orsay Cedex, France

^{||}Chemical Resources Laboratory and Integrated Research Institute, Tokyo Institute of Technology, 4259 Nagatsuta, Midori-ku, Yokohama 226-8503, Japan

[⊥]Physique des Interactions Ioniques et Moléculaires (PIIM), UMR-CNRS 7345 Aix-Marseille Université, Avenue Escadrille Normandie-Niémén, 13397 Marseille Cedex 20, France

ABSTRACT: The gas phase structure of 2-aminophenol has been investigated using UV–UV as well as IR–UV hole burning spectroscopy. The presence of a free OH vibration in the IR spectrum rules out the contribution of the *cis* isomer, which is expected to have an intramolecular H-bond, to the spectra. The excited state lifetimes of different vibronic levels have been measured with pump–probe picosecond experiments and are all very short (35 ± 5) ps as compared to other substituted phenols. The electronic states and active vibrational modes of the *cis* and *trans* isomers have been calculated with *ab initio* methods for comparison with the experimental spectra. The Franck–Condon simulation of the spectrum using the calculated ground and excited state frequencies of the *trans* isomer is in good agreement with the experimental one. The very short excited state lifetime of 2-aminophenol can then be explained by the strong coupling between the two first singlet excited states due to the absence of symmetry, the geometry of the *trans* isomer being strongly nonplanar in the excited state.



I. INTRODUCTION

Excited state hydrogen detachment (ESHD) is a key mechanism in the photochemistry of photoacid aromatic molecules containing OH, NH, or SH groups or heterocyclic NH groups, and excited state hydrogen transfer (ESHT) is the equivalent mechanism in clusters containing these aromatic molecules with H acceptor molecules.^{1,2} These ESHD and ESHT reactions have been computationally predicted and experimentally confirmed in many systems including phenol (PhOH),^{3–9} substituted PhOHs (XPhOH),^{10–14} thiophenol,¹⁵ pyrrole,^{16,17} indole,^{18–20} and substituted-indoles.²¹

The broadly accepted mechanism for ESHD/T suggests that the X–H (X = O, N, S) bond fission takes place on a potential energy surface of $\pi\sigma^*$ character, dissociative along the X–H coordinate. However, in most of the molecules, the $S_2(\pi\sigma^*)$ state locates significantly higher in energy than the $S_1(\pi\pi^*)$ state, which provides most of the transition strength. The $\pi\pi^*$ state is bound along the X–H coordinate, which results in an avoided crossing with the $\pi\sigma^*$ state at an intermediate X–H distance. Therefore, at low excitation energy the $\pi\sigma^*$ state is reached by H atom tunneling through the barrier on the shoulder of the $\pi\pi^*/\pi\sigma^*$ conical intersection.^{1,14} In most of the cases studied up to now, the C_s symmetry is conserved in the excited state so that the coupling between the $\pi\pi^*$ and $\pi\sigma^*$ states necessitates some symmetry breaking via vibrational

coupling as evidenced by the vibrational distribution in the phenoxy radical after excited state H atom loss in PhOH³ and substituted X–PhOH (X = F, Cl, and CH₃)⁹ and corroborated by recent theoretical calculations.²²

Phenol (PhOH) is a prototype of photoacid aromatic molecule that undergoes ESHD upon excitation of the isolated molecule, ESHT to the solvent when solvated in small PhOH(solvent)_n clusters,^{23,24} or concerted electron and proton transfer reaction when it is hydrogen-bonded to another photoacid aromatic molecule such as 7-azaindole.²⁵ In a series of X–PhOH derivatives (X = F and CH₃) and their 1:1 complexes with NH₃, it has been demonstrated a correlation between the excited state lifetime and the energy gap between the $\pi\pi^*$ and $\pi\sigma^*$ states as long as the excited state maintains the C_s symmetry.¹⁴ However, the lifetime of the *cis*-*o*-F-PhOH–(NH₃) complex was reported to be much shorter than the prediction based on the $\pi\pi^*/\pi\sigma^*$ energy gap model, which can be related to the existence of an important out-of-plane distortion of the C–F bond in the S_1 excited state, as revealed by quantum chemical calculations. This distortion reduces the symmetry from C_s to C_1 and the discrimination between $\pi\pi^*$

Received: November 21, 2013

Revised: February 26, 2014

Published: February 26, 2014



and $\pi\sigma^*$ turns unacceptable, the excited states are expected to be completely mixed, and consequently, the ESHT reaction becomes faster.

It has also been recently reported that the excited state lifetime of free catechol is in the order of 5–11 ps, which is much shorter than the excited state lifetime of bare PhOH (>1.2 ns).^{26–28} The authors also suggested that this short lifetime is a direct consequence of the nonplanar S_1 excited state minimum structure (C_1 symmetry) in catechol.

Aniline is another relevant aromatic molecule that also presents a low lying $\pi\sigma^*$ state located on the NH_2 group²⁹ that leads to ESHD at higher excitation energies (photon wavelength below 250 nm).^{30,31}

Particularly interesting is the aminophenol (NH_2PhOH) molecule because it is a prototype for studying the interactions and the excited state dynamics of the structurally related amino acid tyrosine and the neurotransmitter dopamine, in which the excited states are likely to be highly perturbed due to the presence of both the NH_2 and the OH groups. This molecule is an appealing system for spectroscopic study because it exhibits both structural and rotational isomerism, determined by the relative positions and conformations of the amino and hydroxyl substituents. The *ortho*-aminophenol (2-aminophenol) case is especially motivating because the close proximity of the substituents provides potential for the formation of $\text{NH}\cdots\text{O}$ or $\text{OH}\cdots\text{N}$ intramolecular hydrogen bonds. In this molecule, two stable structures are expected (see Figure 3), the *cis* isomer in which OH group interacts by a H-bond with the N lone electron pair of the NH_2 group and the *trans* isomer in which the intermolecular H-bond does not exist. Fujii and co-workers³² have performed nonresonant ionization detected (NID) spectroscopy and showed that under their supersonic jet conditions only the *trans* isomer is observed. The authors suggested that in the *trans* isomer the NH_2 group adopts an aniline-like geometry, which allows for maximum resonance stabilization between the N lone electron pair and the π^* orbitals of the ring, and this stabilization is stronger than the one produced by the H-bond in the *cis* isomer. Therefore, the *trans* isomer is the most stable one.

The C_2 symmetry is therefore broken as a consequence of the aniline-like pyramidalization in the *trans* isomer and of the intermolecular H-bond in the *cis* isomer, if it exists. This symmetry breaking is expected to strongly affect the $\pi\pi^*/\pi\sigma^*$ conical intersection as in the case of catechol^{26–28} and *cis*-*o*-F-PhOH(NH_3) complex.¹⁴ Therefore, the role of the symmetry breaking on the excited state lifetime can be investigated in such a molecule.

In this work, we combined REMPI ($1 + 1'$) spectroscopy with picosecond and nanosecond pulses, UV–UV and IR–UV hole burning spectroscopies, and excited state lifetime determination by picoseconds pump–probe experiments with *ab initio* calculation on the ground and excited states of *o*-aminophenol, to characterize its structure and the effect of the symmetry on the excited state dynamics.

II. METHODS

A. Experimental Section. The experiments have been conducted in two laboratories.

Picosecond measurements were performed in Orsay, where jet-cooled molecules were generated by expanding neat He or Ne, that has passed over a reservoir containing 2-aminophenol maintained at a temperature varying from 65 to 90 °C. The 2-aminophenol (from Sigma-Aldrich Chemie S.A.R.L.) was used

without further purification. The backing pressure was typically 1 bar and the gaseous mixture was expanded to vacuum through a 300 μm diameter pulsed nozzle (solenoid general valve, series 9). The skimmed free jet was crossed at right angle by the copropagated excitation and ionization laser beams, 10 cm downstream from the nozzle. The produced ions were accelerated perpendicularly to the jet axis toward a micro-channel plates detector located at the end of a 1.5 m field-free flight tube.

The third harmonic (355 nm) output of a mode-locked picosecond Nd:YAG laser (EKSPLA-SL300) was split into two parts in order to pump two optical parametric amplifiers (OPA) with second harmonic generation (SHG) systems (EKSPLA-PG411) to obtain tunable UV light. One of the systems was used as the excitation laser (ν_1) tuned on the different transitions of the molecule. The energy of the ν_1 laser was attenuated to preclude one-color two-photon ionization. The other OPA-SHG system was tuned to 310 nm and used as the ionization laser (ν_2) keeping the energy to approximately 120 $\mu\text{J}/\text{pulse}$. The temporal shapes of both pulses were determined in the fitting procedure to be Gaussian having full width at half height (fwhh) of 10 ps, while the spectral line width was 15 cm^{-1} . Both laser pulses were optically delayed between –350 and 1350 ps by a motorized stage.

The nanosecond experiments were performed in Tokyo Tech. The experimental conditions in Tokyo were almost the same as in Orsay, except that the reservoir temperature was kept fixed at 70 °C, and the jet was produced by expanding 2 bar of net Ar into the vacuum chamber. The generated cations were detected as mentioned above.

For the UV–UV and IR–UV hole burning (HB) spectroscopy experiments, a probe laser, ν_p , was fixed to a certain band observed in the REMPI spectrum and the generated ions were detected. Prior to ν_p , an intense burn laser, ν_b , was fired and scanned to depopulate the ground state probed by the ν_p laser. The electronic spectrum of a single specific isomer was measured by scanning ν_b while monitoring the ion current arising from ν_p . In the same way, changing the UV laser ν_b by a tunable IR laser, the isomer-selected vibrational spectra were determined.

The probe laser, ν_p , and the burn laser, ν_b , were obtained by frequency-doubled dye lasers (Lumonics: HD-500, Sirah: Cobra-Stretch), which were pumped by the third harmonics of Nd^{3+} :YAG lasers (LOTIS-TII: LS-2137, Continuum: Surelite I-10). The tunable IR laser, ν_{IR} , for the IR dip spectroscopy was generated by difference-frequency mixing, using the output of a dye laser (Fine Adjustment: Pulsare-S Pro) pumped by a 50% output of a second harmonic of a Nd^{3+} :YAG laser (Spectra Physics: PRO-230) and a 10% output of the second harmonic in a LiNbO_3 crystal.

B. Calculations. Calculations were performed for the *cis* and *trans* isomers of 2-aminophenol with the TURBOMOLE program package,³³ making use of the resolution-of-the-identity (RI) approximation for the evaluation of the electron-repulsion integrals³⁴ in the MP2 and CC2 calculations in Orsay on the GMPCS cluster. The ground-state equilibrium geometries were determined using the MP2 method. Vertical excitation energies and oscillator strengths were calculated at the ground-state equilibrium geometry with the CC2 method,³⁵ using Dunning's correlation-consistent split-valence double- ζ basis set with polarization functions on all atoms (aug-cc-pVDZ).³⁶ In addition to the ground-state geometry optimization and vertical excitation energy calculations, the geometry of the lowest

excited state was also optimized at the RI-CC2 level with the aug-cc-pVDZ basis set.

The vibrational frequencies in the ground and excited states have been calculated and the vibronic spectrum simulated using the PGOPHER software³⁷ for the Franck–Condon analysis.

III. RESULTS

A. Experimental Section. REMPI and Hole Burning (UV–UV and IR–UV) Spectra. The REMPI spectrum of 2-aminophenol (shown in Figure 1) was recorded with both,

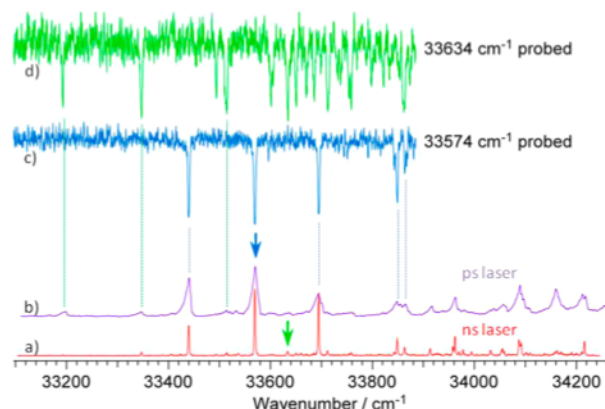


Figure 1. REMPI excitation spectrum recorded with (a) ns laser with 0.08 cm^{-1} resolution; (b) ps laser with 15 cm^{-1} resolution. UV–UV hole burning spectrum pumping the band at (c) 33574 cm^{-1} (blue arrow) and (d) the small band at 33634 cm^{-1} (green arrow).

nanosecond and picosecond laser pulses. The spectrum is characterized by a vibrational progression of 130 cm^{-1} , starting from the band at 33443 cm^{-1} (4.14 eV), which is assigned to the 0–0 transition. The 0–0 transition is not the most intense band, which is an indication of some strong geometry change between S_0 and S_1 . Two weak bands red-shifted by -246 and -96 cm^{-1} from the 0–0 transition are source temperature- and carrier gas-dependent suggesting that they could be hot bands or belong to another isomer.

To confirm the presence of a different isomer or hot bands, the UV–UV HB spectra were measured by fixing the probe laser to the bands centered at 33574 and 33634 cm^{-1} (see arrows in Figure 1). The results are also depicted in Figure 1 and clearly show that the small bands and the intense bands are not coming from the same initial states or species. In addition, the small bands are also associated with a congested group of transitions in the region (33500 – 33900) cm^{-1} .

Further information was obtained from the IR–UV HB spectra presented in Figure 2 for the two species. Both spectra are very similar and exhibit a free OH vibration at $3665.5/3668.8\text{ cm}^{-1}$, ruling out the contribution to the spectra of the cis isomer, which is expected to have an intramolecular H-bond between the H atom of the OH group and the lone electron pair on the N atom of the NH_2 group (Figure 3). The IR spectra are then unequivocally assigned to the trans isomer in both cases.

Excited State Lifetime Measurements. Pump–probe experiments with picosecond laser pulses were performed to determine the excited state lifetime of different vibrational states by pumping on different vibronic transitions and ionizing with 310 nm photons. The results are reported in Table 1.

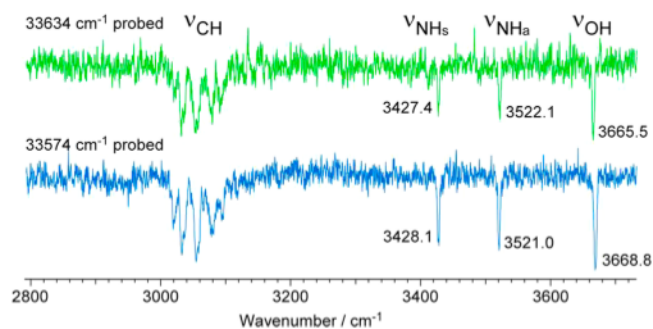


Figure 2. IR–UV hole burning spectra of the two species (isomers or hot bands) probing the band at 33574 cm^{-1} (lower panel) and the small band at 33634 cm^{-1} (upper panel).

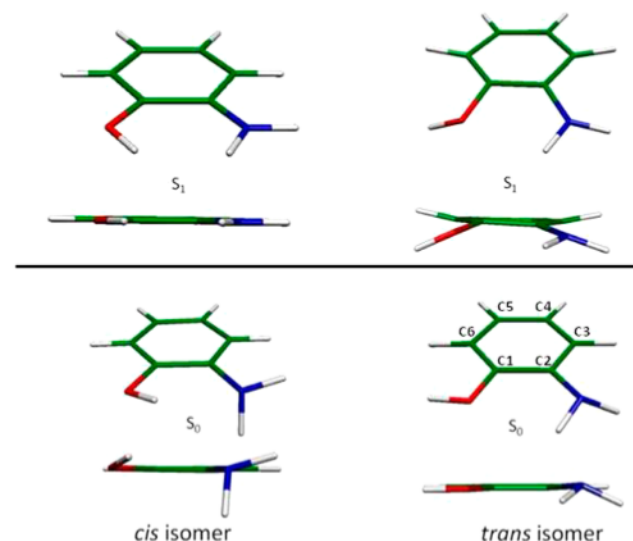


Figure 3. Optimized geometries of cis (left) and trans (right) 2-aminophenol in the ground (S_0) and first excited (S_1) states calculated at the RI-CC2/aug-cc-pVDZ level of theory.

Table 1. Excited State Lifetimes of 2-Aminophenol Recorded by Exciting at Different Vibronic States and Ionizing at 310 nm; the Reported Lifetimes Are the Average of Several Measurements while the Corresponding Errors Are the Standard Deviation of All the Measurements

transition (cm^{-1})	lifetime (ps)	vibrational assignment
-246	36 ± 2	2_1^0
-96	28 ± 2	2_1^1
0 (33443 cm^{-1})	34 ± 2	0_0^0
132	33 ± 3	2_0^1
256	55 ± 5	2_0^2
406	27 ± 2	9_0^1
475	34 ± 2	$1_1^1 2_0^{1a}$
520	29 ± 2	$9_0^1 2_0^1$
649	38 ± 2	$9_0^1 2_0^2$
843	36 ± 5	$1S_0^1 2_0^2$

^aThis transition is tentatively assigned.

The excited state lifetimes are very short as compared to those of PhOH and other substituted X–PhOHs,¹⁴ but longer than in catechol.^{26–28} For most of the bands the lifetime is (35 ± 5) ps except for one band at 256 cm^{-1} , which has a longer lifetime of (55 ± 5) ps. The two small red-shifted bands have

the same lifetimes as the two first intense bands and are assigned to hot bands starting from vibrational excited levels in the ground state and leading to the same vibrational levels in the excited state (see discussion section).

B. Calculations. The ground state geometries of both, the cis and the trans isomers have been calculated at the RI-MP2 and RI-CC2 level of theory using the aug-cc-pVDZ basis set. The trans and cis isomers are almost isoenergetical at this level of calculation ($\Delta E < -0.001$ eV at the MP2 level, and $\Delta E = 0.002$ eV at the CC2 level). However, when the zero-point energy (ZPE) is taken into account, the trans isomer becomes more stable by 0.013 eV at the MP2 level and 0.015 eV at the CC2 level than the cis isomer, while the energy barrier for the isomerization is 0.12 eV. This is different from the result of the B3LYP/6-311++G(2d,2p) calculations predicting that only the trans isomer is a true minimum.³²

The ground state geometry of both isomers is shown in Figure 3. The geometry of the trans isomer stays essentially planar except for the hydrogen atoms of the NH₂ group, which is bent by 23° being smaller than the angle value (around 37°) in aniline.³⁸ For the cis isomer, the hydrogen bond forces the rotation of the NH₂ group along the CN axis, and the hydrogen of the OH group is pushed out of plane. The rotation of the NH₂ group induces a deconjugation of the N lone electron pair. Therefore, the significant driving force that favors the trans isomer is the strong π -donation from the NH₂ group to the ring, which cannot be compensated by the formation of a relatively strong OH...N H-bond in the cis isomer in agreement with previous work.³²

The vertical energy of the S₁ and S₂ states at the optimized geometry of the S₀ state were calculated for both isomers at the RI-CC2/aug-cc-pVDZ level of theory (upper panel of Table 2). In both cases, the two first excited states are very close in energy.

Table 2. Ground and Excited State Energies (in eV) and Oscillator Strengths Calculated at the RI-CC2/aug-cc-pVDZ Level of Theory for the cis and trans Isomers of 2-Aminophenol

	cis		trans	
	energy (eV)	oscillator strength	energy (eV)	oscillator strength
Ground State Optimized Geometry				
S0 (ZPE included)	0.015		0.00	
S0–S1 (vertical transition, without δ ZPE)	4.756	4.3×10^{-02}	4.542	4.8×10^{-02}
S0–S2 (vertical transition, without δ ZPE)	4.996	8.9×10^{-03}	4.638	2.1×10^{-02}
Excited State Optimized Geometry				
S0	0.59		0.46	
S1	4.07		4.19	
S0–S1 (adiabatic transition including δ ZPE)	3.93		4.03	(4.15 eV exp.)
S2	4.93		4.75	

The optimization of the first excited state was performed at the RI-CC2/aug-cc-pVDZ level of theory and led to a strong stabilization of the energy by 0.69 eV for the cis isomer and 0.35 eV for the trans isomer (lower panel of Table 2). The energy of the adiabatic transition is calculated as the difference between the energy of the S₁ state at the optimized geometry of

the S₁ state minus the energy of the S₀ state at the optimized geometry of the S₀ state minus the difference in zero-point energy between the ground and the excited states (δ ZPE). The difference in ZPE between ground and excited states is about 0.15 eV for both isomers as in other aromatic molecules.¹⁴ The origins of the S₁ ← S₀ electronic transition for the trans and cis isomers are then calculated at 4.03 and 3.93 eV, respectively.

The optimized geometries at the S₁ state of both isomers are shown in the upper panel of Figure 3. For the trans isomer, the S₁ optimization leads to a geometry in which the NH₂ group becomes more planar, the OH bond comes out of the ring plane by 16°, and the C3H and C6H bonds also get out of plane by ca. –12°. In the case of the cis isomer, the first excited state optimization leads to a planar geometry.

For both isomers the oscillator strengths (Table 2) of the two first excited state are similar (within a factor of 5) in comparison with PhOH for which the oscillator strength of the S₁($\pi\pi^*$) state is 100 times larger than for the S₂($\pi\sigma^*$) state.³⁹ The similarity of these oscillator strengths reflects the strong mixing between the S₁ and S₂ states and makes it difficult to classify the electronic states using the C_s symmetry labels.

To get more insight into the character of the excited states, the orbitals involved in the S₁ ← S₀ and S₂ ← S₀ transitions of the trans isomer are depicted in Figure 4. Although the analysis

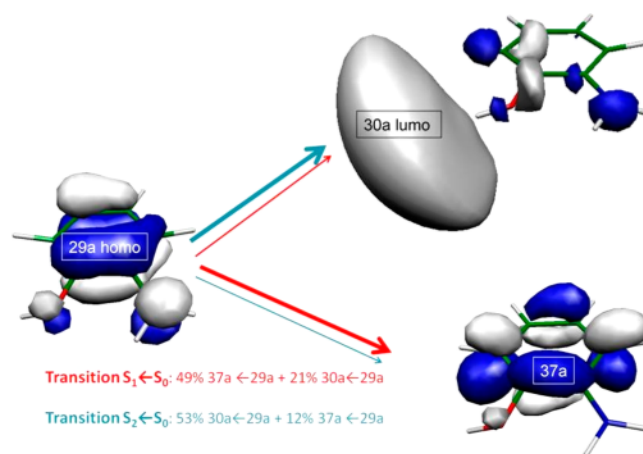


Figure 4. Orbitals involved in the S₁ ← S₀ and S₂ ← S₀ electronic transitions for the *trans*-2-aminophenol, calculated at the RI-CC2/aug-cc-pVDZ level.

of these orbitals indicates that the S₁ state has a main $\pi\pi^*$ character and the S₂ state is mainly of $\pi\sigma^*$ character with the σ^* orbital on the OH group, these states are strongly mixed since the planar symmetry is not conserved.

IV. DISCUSSION

A. Assignment of the observed transitions. The IR–UV hole burning spectrum, recorded by probing one of three most intense vibronic transition at 33 574 cm⁻¹, shows a band at 3668.8 cm⁻¹ that can be assigned to the free OH stretching. Thus, the OH group is not H-bonded and the main bands are associated to the trans isomer. Indeed, for the cis isomer the OH vibration is calculated to be shifted by more than 200 cm⁻¹ as compared to the trans isomer, due to the H-bond between this group and the NH₂ group. The corresponding IR–UV hole burning spectrum (Figure 2), recorded by probing a transition at 33 634 cm⁻¹ associated with the two weak bands observed to the red of the main progression, is very similar to that of the

main bands and thus has also been assigned to the same isomer. Therefore, the small weak red-shifted transitions are assigned to hot bands built on the $\nu = 1$ level of the ν_2 (2_1^0) torsional mode (vide infra) in the ground state of the trans isomer. The very small change in the ν_{OH} frequency is probably due to anharmonic coupling between the ν_{OH} and some ring deformations. Additionally, the origin of the electronic transition for the trans isomer is calculated at 4.03 eV, in good agreement with the experimentally observed origin at 4.15 eV.

The excitation spectra for the cis and trans isomer were simulated using the calculated ground and excited state frequencies and the PGOPHER program³⁷ to compute the Franck–Condon factors. The stick spectrum obtained was convoluted with a Gaussian function of 10 cm^{-1} width.

The simulated and experimental spectra are shown all together in Figure 5 for comparison. As expected from the

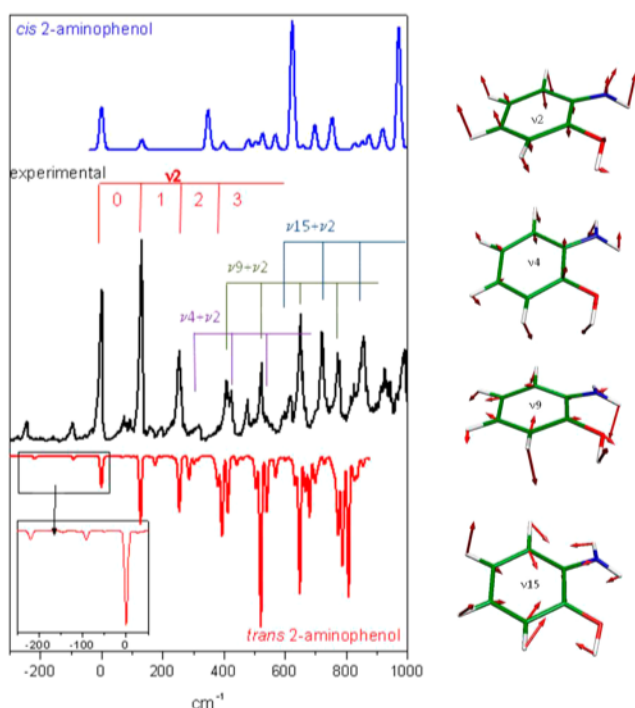


Figure 5. Left panel: simulated spectra using the ground and excited state frequencies calculated at the RI-CC2/aug-cc-pVDZ level for the cis isomer (blue), for the trans isomer with a scaling factor of 0.82 (red), and experimental spectrum (black). The assignment of the vibrational bands is also shown on top of the experimental spectrum. Right panel: Scheme of the vibrational modes involved in the spectrum.

experimental results, there is a poor match between the simulated spectrum for the cis isomer (in blue) and the experimental one, while the matching is reasonably good with the simulated spectrum of the trans isomer (in red) applying a scaling factor of 0.82 as previously used in protonated indole.⁴⁰

Using the simulated spectrum, the vibrational bands observed can be assigned to progressions built on the ν_2 mode involving NH_2 out-of-plane motions (Figure 5, right panel), starting from the 0_0^0 , 4_0^1 , 9_0^2 , and 15_0^3 levels. Note that the ν_9 mode also involves out-of-plane motions of the NH_2 and OH groups, which correspond to the change in geometry between ground and excited state.

These Franck–Condon calculations show a drastic difference for the absolute value of the Franck–Condon factors of both isomers, being the values for the cis isomer around 500 times smaller than those for the trans isomer. This is due to a bigger change in the excited state geometry of the cis isomer as a consequence of its geometry constraint. Thus, assuming an equal population of both isomers and owing to the signal-to-noise ratio of the experiment, the cis isomer is indiscernible and nothing can be concluded about its intrinsic stability in the ground state.

B. Excited State Lifetimes. The excited state lifetime is (35 ± 5) ps for most of the band except for that one at 256 cm^{-1} above the origin of the electronic transition for which it is (55 ± 5) ps. We still do not have any reasonable explanation for this observation.

Considering that the energy gap between the $\pi\pi^*$ and the $\pi\sigma^*$ states ($\delta_{\pi\pi^*-\pi\sigma^*}$) for *trans*-2-aminophenol is 0.1 eV (Table 2), the energy gap law¹⁴ that correlates the excited state lifetime of substituted PhOH with $\delta_{\pi\pi^*-\pi\sigma^*}$ predicts an excited state lifetime in the order of 200 ps for this molecule. This value is longer than the experimental one (35 ± 5) ps, suggesting that an additional effect must be considered to rationalize this short excited state lifetime.

One reason is the planar symmetry breaking in the S_1 state of this molecule as shown in Figure 3, leading to a strong mixing of the $\pi\pi^*$ and $\pi\sigma^*$ states (Figure 4) that enhances the ESHD reaction rate and lead to a very low energy barrier of 0.2 eV (calculated as the minimum energy path along the OH dissociation coordinate). This effect was previously observed in the *cis*-2-fluorophenol(NH_3) complex¹⁴ and in the free catechol molecule.^{26–28} In the former system, the $\delta_{\pi\pi^*-\pi\sigma^*}$ was reported to be 0.623 eV, and the lifetime predicted by the energy gap law of this complex should be in the 2–3 ns range, but the experimental value was 140 ps.¹⁴ In this case quantum chemical calculation revealed an important out-of-plane distortion of the C–F bond in the excited state S_1 that reduces the symmetry from C_s to C_1 , and the discrimination between π^* and σ^* orbitals turns inadequate since the $\pi\pi^*$ and $\pi\sigma^*$ states are expected to be strongly mixed as in the case of the *trans*-2-aminophenol molecule. In the free catechol molecule, the excited state lifetime is in the order of 7–11 ps, and the authors also suggested that this phenomenon is a direct consequence of the nonplanar structure of the molecule in the S_1 excited state.^{26–28}

As highlighted by Stavros and co-workers in a related work,²⁶ it is clear that simple chemical modifications to biological relevant chromophores such as PhOH, induces dramatic effects on the excited state potential energy surface and therefore on the dynamics taking place on it. The substitution in position 2 of the PhOH molecule (ortho substitution) seems to be especially adequate to study this effect.

The gas phase conformational diversity of neurotransmitters (substituted PhOHs with a flexible side chain) has been recently studied by UV–UV and/or IR–UV hole burning spectroscopy.^{41–47} Quite remarkably, DOPA (dihydroxyphenylalanine),^{41,42} noradrenaline,^{43,44} and adrenaline,^{45,46} which are catecholamine neurotransmitters with a catechol ring and different side-chains, have tiny numbers of conformers: 1, 1, and 2 respectively, as determined in the gas phase by UV–UV and/or IR–UV hole burning spectroscopy.

On the contrary, tyrosine,⁴² *m*-tyrosine,⁴¹ and synephrine⁴⁷ have the same side-chain as DOPA and adrenaline, respectively, but with only one phenolic OH group and present multiple

conformers, 8, 14, and 11, respectively. This is another evidence of the importance of the ortho substitution in biological relevant molecules. However, this difference in the number of conformations raises a series of questions about the role of the catechol ring in neurotransmitters, and whether the catecholic OH groups are responsible of locking the molecule into a specific conformation or, alternatively, if the excited state lifetime of other possible conformers are too short to be detected by electronic spectroscopy?

V. CONCLUSIONS

2-Aminophenol shows a well structured vibronic spectrum. UV–UV and IR–UV hole burning spectroscopies definitely show that only the trans isomer is responsible for the excitation spectrum, although the calculations indicate that the cis and trans isomers are close in energy. The Franck–Condon simulation of the spectrum using calculated ground and excited state frequencies for the trans isomer is in good agreement with the experimental one, which gives confidence in the calculated geometries. The very short excited state lifetime of 2-aminophenol can then be explained by the strong coupling between the S_1 and S_2 excited states due to the absence of symmetry, mainly corresponding to an out-of-plane bending of the OH bond.

The comparison of the present results with previous reports on ortho substituted PhOHs suggests that substitution in position 2 of PhOH induces out-of-plane deformations that lead very fast dynamics in the excited states.

■ AUTHOR INFORMATION

Corresponding Author

*(G.A.P.) E-mail: gpino@fcq.unc.edu.ar

Notes

The authors declare no competing financial interest.

■ ACKNOWLEDGMENTS

This work was supported by ECOS–MinCyT cooperation program (A11E02), the CLUPS (Université Paris–Sud 11), the ANR Research Grant (ANR2010BLANC040501), FONCyT, CONICET, and SeCyT–UNC. We acknowledge the use of the computing facility cluster GMPCS of the LUMAT federation (FR LUMAT 2764). The authors thank the reviewers for helpful suggestions.

■ REFERENCES

- (1) Sobolewski, A. L.; Domcke, W.; Dedonder-Lardeux, C.; Jouvét, C. Excited-State Hydrogen Detachment and Hydrogen Transfer Driven by Repulsive $^1\pi\sigma^*$ States: A New Paradigm for Nonradiative Decay in Aromatic Biomolecules. *Phys. Chem. Chem. Phys.* **2002**, *4*, 1093–1100.
- (2) Ashfold, M. N. R.; Cronin, B.; Devine, A. L.; Dixon, R. N.; Nix, M. G. D. The Role of $\pi\sigma^*$ Excited States in the Photodissociation of Heteroaromatic Molecules. *Science* **2006**, *312*, 1637–1640.
- (3) Nix, M. G. D.; Devine, A. L.; Cronin, B.; Dixon, R. N.; Ashfold, M. N. R. High Resolution Photofragment Translational Spectroscopy Studies of the Near Ultraviolet Photolysis of Phenol. *J. Chem. Phys.* **2006**, *125*, 133318(1–13).
- (4) Tseng, C.-M.; Lee, Y. T.; Ni, C. K. H Atom Elimination from the $\pi\sigma^*$ State in the Photodissociation of Phenol. *J. Chem. Phys.* **2004**, *121*, 2459–2461.
- (5) Tseng, C.-M.; Lee, Y. T.; Lin, M.-F.; Ni, C.-K.; Liu, S.-Y.; Lee, Y.-P.; Xu, Z. F.; Lin, M. C. Photodissociation Dynamics of Phenol. *J. Phys. Chem. A* **2007**, *111*, 9463–9470.

- (6) Hause, M. L.; Yoon, Y. H.; Case, A. S.; Crim, F. F. Dynamics at Conical Intersections: The Influence of O–H Stretching Vibrations on the Photodissociation of Phenol. *J. Chem. Phys.* **2008**, *128*, 104307(1–8).

- (7) Iqbal, A.; Cheung, M. S. Y.; Nix, M. G. D.; Stavros, V. G. Exploring the Time-Scales of H-Atom Detachment from Photoexcited Phenol- h_6 and Phenol- d_5 : Statistical vs Nonstatistical Decay. *J. Phys. Chem. A* **2009**, *113*, 8157–8163.

- (8) Iqbal, A.; Pegg, L.-J.; Stavros, V. G. Direct versus Indirect H Atom Elimination from Photoexcited Phenol Molecules. *J. Phys. Chem. A* **2008**, *112*, 9531–9534.

- (9) Dixon, R. N.; Oliver, T. A. A.; Ashfold, M. N. R. Tunnelling Under a Conical Intersection: Application to the Product Vibrational State Distributions in the UV Photodissociation of Phenols. *J. Chem. Phys.* **2011**, *134*, 194303(1–10).

- (10) Tsuji, N.; Ishiuchi, S.-I.; Sakai, M.; Fujii, M.; Ebata, T.; Jouvét, C.; Dedonder-Lardeux, C. Excited State Hydrogen Transfer in Fluorophenol–Ammonia Clusters Studied by Two-Color REMPI Spectroscopy. *Phys. Chem. Chem. Phys.* **2006**, *8*, 114–121.

- (11) Oldani, A. N.; Ferrero, J. C.; Pino, G. A. Effect of the Intermolecular Hydrogen Bond Conformation on the Structure and Reactivity of the *p*-Cresol(H_2O)(NH_3) van der Waals Complex. *Phys. Chem. Chem. Phys.* **2009**, *11*, 10409–10416.

- (12) Sage, A. G.; Oliver, T. A. A.; King, G. A.; Murdock, D.; Harvey, J. N.; Ashfold, M. N. R. UV Photolysis of 4-Iodo-, 4-Bromo-, and 4-Chlorophenol: Competition Between C–Y (Y = Halogen) and O–H Bond Fission. *J. Chem. Phys.* **2013**, *138*, 164318(1–12).

- (13) Oldani, A. N.; Mobbili, M.; Marceca, E.; Ferrero, J. C.; Pino, G. A. Effect of the Vibrational Excitation on the Non-Radiative Deactivation Rate of the S_1 State of *p*-Cresol(NH_3) Complex. *Chem. Phys. Lett.* **2009**, *471*, 41–44.

- (14) Pino, G. A.; Oldani, A. N.; Marceca, E.; Fujii, M.; Ishiuchi, S.-I.; Miyazaki, M.; Broquier, M.; Dedonder, C.; Jouvét, C. Excited State Hydrogen Transfer Dynamics in Substituted Phenols and their Complexes with Ammonia: $\pi\pi^*$ – $\pi\sigma^*$ Energy Gap Propensity and ortho-Substitution Effect. *J. Chem. Phys.* **2010**, *133*, 124313(1–12).

- (15) Oliver, T. A. A.; King, G. A.; Tew, D. P.; Dixon, R. N.; Ashfold, M. N. R. Controlling Electronic Product Branching at Conical Intersections in the UV Photolysis of para-Substituted Thiophenols. *J. Phys. Chem. A* **2012**, *116*, 12444–12459 and references therein.

- (16) Cronin, B.; Nix, M. G. D.; Qadiri, R. H.; Ashfold, M. N. R. High Resolution Photofragment Translational Spectroscopy Studies of the Near Ultraviolet Photolysis of Pyrrole. *Phys. Chem. Chem. Phys.* **2004**, *6*, 5031–5041.

- (17) Rubio-Lago, L.; Amaral, G. A.; Oldani, A. N.; Rodríguez, J. D.; González, M. G.; Pino, G. A.; Bañanares, L. Photodissociation of Pyrrole–Ammonia Clusters by Velocity Map Imaging: Mechanism for the H-Atom Transfer Reaction. *Phys. Chem. Chem. Phys.* **2011**, *13*, 1082–1091.

- (18) Lin, M.-F.; Tseng, C.-M.; Lee, Y. T.; Ni, C.-K. Photodissociation Dynamics of Indole in a Molecular Beam. *J. Chem. Phys.* **2005**, *123*, 124303(1–5).

- (19) Lin, M.-F.; Tzeng, C.-M.; Dyakov, Y. A.; Ni, C.-K. Photostability of Amino Acids: Internal Conversion Versus Dissociation. *J. Chem. Phys.* **2007**, *126*, 241104(1–5).

- (20) Nix, M. G. D.; Devine, A. L.; Cronin, B.; Ashfold, M. N. R. High Resolution Photofragment Translational Spectroscopy of the Near UV Photolysis of Indole: Dissociation via the $^1\pi\sigma^*$ State. *Phys. Chem. Chem. Phys.* **2006**, *8*, 2610–2618.

- (21) Oliver, T. A. A.; King, G. A.; Ashfold, M. N. R. Position Matters: Competing O–H and N–H Photodissociation Pathways in Hydroxy- and Methoxy-Substituted Indoles. *Phys. Chem. Chem. Phys.* **2011**, *13*, 14646–14662.

- (22) Xu, X.; Yang, K. R.; Truhlar, D. G. Diabatic Molecular Orbitals, Potential Energies, and Potential Energy Surface Couplings by the 4-Fold Way for Photodissociation of Phenol. *J. Chem. Theory Comput.* **2013**, *9*, 3612–3625.

- (23) Ishiuchi, S.-I.; Sakai, M.; Daigoku, K.; Hashimoto, K.; Fujii, M. Hydrogen Transfer Dynamics in a Photoexcited Phenol/Ammonia

(1:3) Cluster Studied by Picosecond Time-Resolved UV-IR-UV Ion Dip Spectroscopy. *J. Chem. Phys.* **2007**, *127*, 234304(1–8) and references therein.

(24) Pino, G. A.; Grégoire, G.; Dedonder-Lardeux, C.; Jovet, C.; Martrenchard, S.; Solgadi, D. A Forgotten Channel in the Excited State Dynamics of Phenol–(Ammonia)_n Clusters: Hydrogen Transfer. *Phys. Chem. Chem. Phys.* **2000**, *2*, 893–900.

(25) Capello, M. C.; Broquier, M.; Dedonder-Lardeux, C.; Jovet, C.; Pino, G. A. Fast Excited State Dynamics in the Isolated 7-Azaindole-Phenol H-Bonded Complex. *J. Chem. Phys.* **2013**, *138*, 054304(1–9).

(26) Chatterley, A. S.; Young, J. D.; Townsend, D.; Zurek, J. M.; Paterson, M. J.; Roberts, G. M.; Stavros, V. G. Manipulating Dynamics with Chemical Structure: Probing Vibrationally-Enhanced Tunnelling in Photoexcited Catechol. *Phys. Chem. Chem. Phys.* **2013**, *15*, 6879–6892.

(27) Weiler, M.; Miyazaki, M.; Féraud, G.; Ishiuchi, S.-I.; Dedonder, C.; Jovet, C.; Fujii, M. Unusual Behavior in the First Excited State Lifetime of Catechol. *J. Phys. Chem. Lett.* **2013**, *4*, 3819–3823.

(28) Livingstone, R. A.; Thompson, J. O. F.; Iljina, M.; Donaldson, R. J.; Sussman, B. J.; Paterson, M. J.; Townsend, D. Time-Resolved Photoelectron Imaging of Excited State Relaxation Dynamics in Phenol, Catechol, Resorcinol, and Hydroquinone. *J. Chem. Phys.* **2012**, *137*, 184304(1–17).

(29) Ebata, T.; Minejima, C.; Mikami, N. A New Electronic State of Aniline Observed in the Transient IR Absorption Spectrum from S₁ in a Supersonic Jet. *J. Phys. Chem. A* **2006**, *106*, 11070–11074.

(30) Tseng, C.-M.; Dyakov, Y. A.; Huang, C.-L.; Mebel, A. M.; Lin, S.-H.; Lee, Y. T.; Ni, C.-K. Photoisomerization and Photodissociation of Aniline and 4-Methylpyridine. *J. Am. Chem. Soc.* **2004**, *126*, 8760–8768.

(31) Roberts, G. M.; Williams, C. A.; Young, J. D.; Ullrich, S.; Paterson, M. J.; Stavros, V. G. Unraveling Ultrafast Dynamics in Photoexcited Aniline. *J. Am. Chem. Soc.* **2012**, *134*, 12578–12589.

(32) Robinson, T. W.; Kjaergaard, H. G.; Ishiuchi, S.-I.; Shinzaki, M.; Fujii, M. Vibrational Overtone Spectroscopy of Jet-Cooled Aminophenols as a Probe for Rotational Isomers. *J. Phys. Chem. A* **2004**, *108*, 4420–4427.

(33) Ahlrichs, R.; Bär, M.; Häser, M.; Horn, H.; Kölmel, C. Electronic Structure Calculations on Workstation Computers: The Program System Turbomole. *Chem. Phys. Lett.* **1989**, *162*, 165–169.

(34) Weigend, F.; Häser, M.; Patzelt, H.; Ahlrichs, R. RI-MP2: Optimized Auxiliary Basis Sets and Demonstration Efficiency. *Chem. Phys. Lett.* **1998**, *294*, 143–152.

(35) Christiansen, O.; Koch, H.; Jørgensen, P. The 2nd-Order Approximate Coupled-Cluster Singles and Doubles Model CC2. *Chem. Phys. Lett.* **1995**, *243*, 409–418.

(36) Woon, D. E.; Dunning, T. H. Gaussian Basis Sets for use in Correlated Molecular Calculations. III. The Atoms Aluminum through Argon. *J. Chem. Phys.* **1993**, *98*, 1358–1371.

(37) Western, C. M. PGOPHER, a Program for Simulating Rotational Structure, V 7.0.101. <http://pgopher.chm.bris.ac.uk> (accessed Oct 7, 2013).

(38) Lister, D. G.; Tyler, J. K.; Høg, J. H.; Larsen, N. W. The Microwave Spectrum, Structure and Dipole Moment of Aniline. *J. Mol. Struct.* **1974**, *23*, 253–264.

(39) Carrera, A.; Nielsen, I. B.; Çarçabal, P.; Dedonder, C.; Broquier, M.; Jovet, C.; Domcke, W.; Sobolewski, A. L. Biradicalic Excited States of Zwitterionic Phenol–Ammonia Clusters. *J. Chem. Phys.* **2009**, *130*, 024302(1–8).

(40) Alata, I.; Bert, J.; Broquier, M.; Dedonder, C.; Féraud, G.; Grégoire, G.; Soorkia, S.; Marceca, E.; Jovet, C. Electronic Spectra of the Protonated Indole Chromophore in the Gas Phase. *J. Phys. Chem. A* **2013**, *117*, 4420–4427.

(41) Mitsuda, H.; Miyazaki, M.; Nielsen, I. B.; Çarçabal, P.; Dedonder, C.; Jovet, C.; Ishiuchi, S.; Fujii, M. Evidence for Catechol Ring-Induced Conformational Restriction in Neurotransmitters. *J. Chem. Phys. Lett.* **2010**, *1*, 1130–1133.

(42) Ishiuchi, S.; Mitsuda, H.; Asakawa, T.; Miyazaki, M.; Fujii, M. Conformational Reduction of DOPA in the Gas Phase Studied by

Laser Desorption Supersonic Jet Laser Spectroscopy. *Phys. Chem. Chem. Phys.* **2011**, *13*, 7812–7820.

(43) Snoek, L. C.; Van Mourik, T.; Çarçabal, P.; Simons, J. P. Neurotransmitters in the Gas Phase: Hydrated Noradrenaline. *Phys. Chem. Chem. Phys.* **2003**, *5*, 4519–4526.

(44) Snoek, L. C.; Van Mourik, T.; Simons, J. P. Neurotransmitters in the Gas Phase: a Computational and Spectroscopic Study of Noradrenaline. *Mol. Phys.* **2003**, *101*, 1239–1248.

(45) Çarçabal, P.; Snoek, L. C.; Van Mourik, T. A Computational and Spectroscopic Study of the Gas-Phase Conformers of Adrenaline. *Mol. Phys.* **2005**, *103*, 1633–1639.

(46) Van Mourik, T. The Shape of Neurotransmitters in the Gas Phase: A Theoretical Study of Adrenaline, Pseudoadrenaline, and Hydrated Adrenaline. *Phys. Chem. Chem. Phys.* **2004**, *6*, 2827–2837.

(47) Ishiuchi, S.-I.; Asakawa, T.; Mitsuda, H.; Miyazaki, M.; Chakraborty, S.; Fujii, M. Gas-Phase Spectroscopy of Synephrine by Laser Desorption Supersonic Jet Technique. *J. Phys. Chem. A* **2011**, *115*, 10363–10369.

